TITLE: Ultrahigh-Sensitive Far-Infrared Detection Based on Quantum Hall
Devices

DISTRIBUTION: Approved for public release, distribution unlimited
Availability: Hard copy only.

This paper is part of the following report:

TITLE: Nanostructures: Physics and Technology International Symposium
[6th] held in St. Petersburg, Russia on June 22-26, 1998 Proceedings

To order the complete compilation report, use: ADA406591

The component part is provided here to allow users access to individually authored sections
of proceedings, annals, symposia, etc. However, the component should be considered within
the context of the overall compilation report and not as a stand-alone technical report.

The following component part numbers comprise the compilation report:
ADP012712 thru ADP012852

Ultrahigh-sensitive far-infrared detection based on quantum Hall devices

S. Komiyama†, H. Hirai†, O. Astafiev‡ Y. Kawano†, T. Sawada†
and T. Sakamoto§

† Department of Basic Science, The University of Tokyo, Komaba
‡Japan Science and Technology Corportation (JST)
§ NEC Basic Research Laboratory, Tsukuba

Abstract.   Extremely high sensitive detection of far-infrared waves associated with cyclotron resonance in two-dimensional electron gas systems is described based on two sets of experiments. One set of experiments studies a bolometer effect of the integer quantum Hall effects. Another set of experiments is based on the bolometer effect of Coulomb blockade oscillations in a quantum dot. In addition, prediction is made on the single photon detection when a quantum dot is excited via cyclotron resonance.

1 Introduction

High-mobility two dimensional electron gas (2DEG) systems strongly absorb far-infrared (FIR) waves upon cyclotron resonance (CR) in high magnetic fields [1]. Combining the CR with some physical parameter of the system that is influenced by the CR, one can construct a magnetically-tunable high-sensitive FIR detector based on a 2DEG system. In this report we discuss three different mechanisms. In Sec. 2, long Hall bars in the regime of integer quantum Hall effects (IQHE) are shown to serve as an extremely sensitive detector. Section 3 describes even more sensitive detection based on a quantum dot, where a 2DEG absorbs the FIR waves while the quantum dot weakly coupled through tunneling to the 2DEG senses a change in the effective electron temperature of the 2DEG. In Sec.4, we argue that the single photon detection of the FIR waves may be possible when the dot is excited by CR. Relevant experimental results of transport measurements, which we believe to infer the realizability of the mechanism, will be described.

2 Quantum Hall-bars

FIR-photoresponse in 2DEG Hall bars is known to take place via three different mechanisms at present: a bulk effect [2, 3] and two types of edge effects [3, 4]. We focus our attention on the bulk effect below.

One of the remarkable characteristics of 2DEG systems in high magnetic fields is the vanishing of the longitudinal resistance in the IQHE. When a 2DEG system in the IQHE regime is illuminated with FIR waves of the photon energy equal to the Landau level energy spacing, electrons and holes are excited via CR to cause finite longitudinal resistance ΔR_{xx}. We note that the induced resistivity, $\Delta\rho_{xx}$, is determined by the power density of incident waves. Therefore, the photo-induced voltage detected in a given conductor under a given intensity of illumination is proportional to the aspect ratio
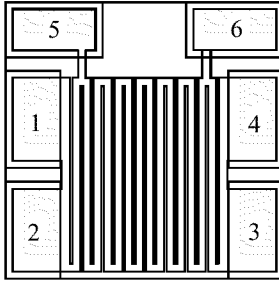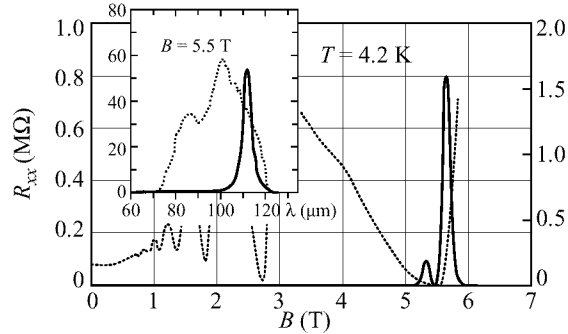
Fig. 1. Illustration of a long Hall bar.

Fig. 2. Shubunikov de-Haas oscillations (the dotted line) and the FIR photoresponse (the solid line). The inset shows a spectral response (the solid line) studied by scanning wavelength of the tunable Ge-laser. The dotted line indicates the dependence of the laser power on the wavelength.

L/W of the conductor used; viz., $\Delta V_{xx} = \Delta R_{xx}I = (L/W)\Delta\rho_{xx}I$, where I is the current and L and W are the length and the width of the conductor.

In dissipative conductors with $R_{xx} \neq 0$, large aspect ratio does not lead to better detector-performance because the noise power density, $Sv = 4k_BT(R_H + R_{xx}) + 2eR_{xx}^2I$, increases as well with increasing L/W, where R_H is the Hall resistance. In the IQHE regime, where $R_{xx} = 0$ and R_H takes on a fixed quantized value $h/\nu e^2$, photosignal grows without the cost of noise. Hence, long Hall bars serve as an extremely high sensitive FIR detector.

FIR photoresponse has been studied in long Hall bars fabricated on high-mobility GaAs/AlGaAs single heterostructure crystals with 4.2 K-electron mobilities, μ_H, ranging from 7 to 100 m^2/Vs. To achieve extremely large aspect ratio ($L/W = 300 \sim 50,000$), the Hall bars are formed zigzag in a square of 4×4 mm^2 as shown in Fig. 1.

Sharp and strong photoresponse occurs at cyclotron resonance [3]. The inset of Fig. 2 shows an example taken on a Hall bar with $L/W = 300$ ($L = 60$ mm, $W = 200\,\mu$m and $\mu_H = 80$ m^2/Vs) placed in a magnetic field close to the $\nu = 2$ IQHE state. The sample is illuminated by the light from a tunable p-type Germanium laser [5] after sufficient attenuation. The spectral purity of the incident radiation $\Delta\lambda$ is about $2\,\mu$m, and the wavelength is continuously varied over the range $\lambda = 76 \sim 125\,\mu$m.

By using tunable cyclotron-emission from n-InSb hot-electron devices as the source of radiation, it is confirmed that observable photoresponse occurs only in the vicinity of IQHE states ($\nu = 2, 4,$ and 6 with $B = 2 \sim 7$ T). An example is demonstrated in Fig. 2 with a solid line, where magnetic-field dependence of the photoresponse under the broad-band illumination (with a spectral line width of $\Delta\nu = 17$ cm^{-1} centered at $\nu = 70$ cm^{-1}) is displayed. Here the sample is a Hall bar with $L/W = 3340$ ($L = 167$ mm, $W = 50\,\mu$m) fabricated on the same wafer as that of the device for the inset. The current is $3\,\mu$A.

The photoresponse does not form a single peak at the center of the IQHE state but takes two maxima at magnetic-field positions slightly off the center as noted in Fig. 2, and more clearly shown by the solid line in Fig. 3(a).

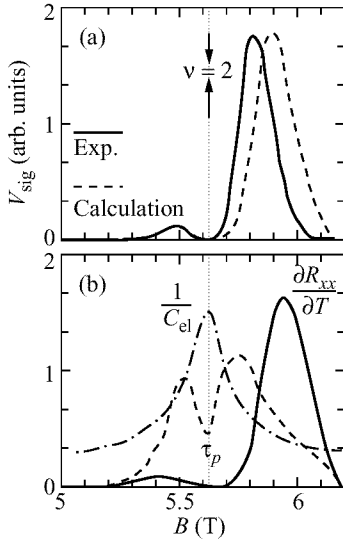This is linked to the fact that (i) the energy of excited electrons and holes is redis-

Fig. 3. (a) Magnetic field dependence of the photoresponse (the solid line) compared with a theoretical values (the broken line). (b) The inverse of the 2DEG heat capacity (the dash-dot line), the temperature derivative of R_{xx} (the solid line) and the time constant of the photoresponse (the dots with a broken line).
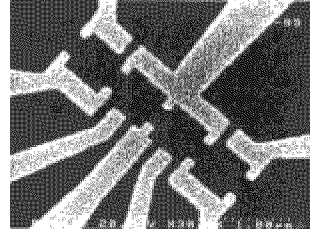

Fig. 4. SEM image of quantum dots studied in the experiments.

tributed to raise the effective electron temperature ΔT_e and (ii) the photoresponse arises primarily from multi-trapping process of heated electrons (holes) between localized and delocalized states. The time constant of the photoresponse is accordingly large, reaching an order of ms.

The photosignal is, most simply, expressed as

$$\Delta R_{xx} = (\partial R_{xx}/\partial T)\Delta T_e \quad \text{with} \quad \Delta T_e = P\tau_E/C_{el}, \tag{1}$$

where P is the rate of energy gain due to CR, τ_E is the energy relaxation time of excited electrons and holes, and C_{el} is the specific heat of the 2DEG. Magnetic-field-dependencies of the relevant quantities are shown together in Fig. 3(b). The temperature derivative of the longitudinal resistance, $\partial R_{xx}/\partial T$, and the time constant of the photoresponse, τ_P, have been experimentally determined. The specific heat, C_{el}, has been theoretically evaluated by assuming a Gaussian-type density of states after Ref. [6]. The broken line in Fig. 3(b) indicates the theoretically expected values, $(\partial R_{xx}/dT)\tau_P/C_{el}$, obtained by multiplying these quantities, which reproduce fairly well the experimental line shape of the photoresponse.

Among the samples studied, the highest responsivity reaches a value of $10^6 \sim 10^7$ V/W in a Hall bar with $L/W = 50,000$ ($W = 4\,\mu$m, $L = 200$ mm and $\mu_H = 80\,\text{m}^2$/Vs) at $B = 5.6$ T ($\nu = 2$ and $\lambda = 130\,\mu$m). The noise equivalent power is roughly estimated to be as low as 1×10^{-13} W/$\sqrt{\text{Hz}}$ (in a 100 Hz-range) at 4.2 K.
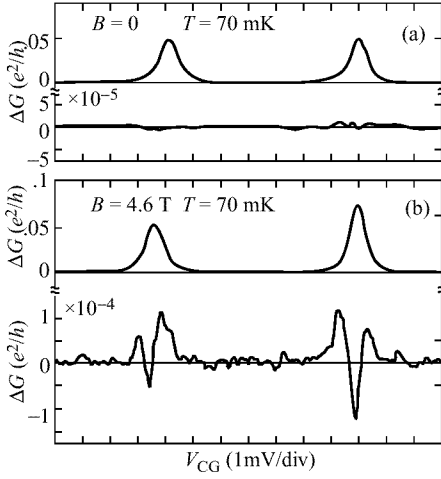
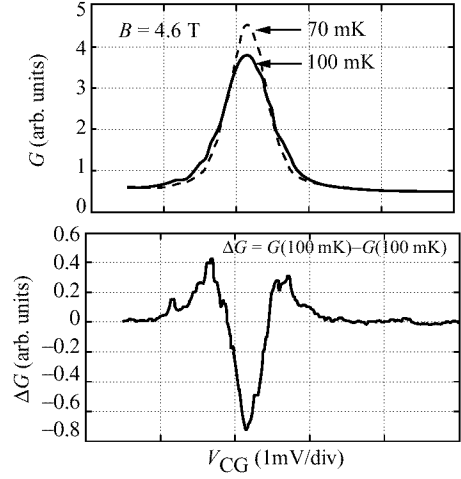**Fig. 5.** Coulomb blockade oscillations and the modulated signal at (a) $B = 0$ and (b) $B = 4.6$ T.

Fig. 6. A Coulomb blockade peak at two different temperatures (the upper) and the difference between the two (the lower).

3   Quantum dots: bolometer effect

When a quantum dot fabricated by lateral confinement of the 2DEG on a Hall bar is weakly coupled through tunneling barriers to the outside 2DEG, the conductance through the dot exhibits Coulomb-blockade oscillations as the number N of the electrons confined within the dot varies due to the voltage on a nearby gate electrode. Since the conductance peak value of the oscillations strongly depends on temperature, the effect of heating the surrounding 2DEG by CR is sensed by the dot in an extremely sensitive way.

Experiments are made by forming one quantum dot on the sample shown in Fig. 4 and applying the voltage of $V_{SD} = 15\,\mu$V to the quantum dot at $T = 70$ mK in the range of magnetic field $0 \leq B \leq 8$ T. Each dot in Fig. 4 is fabricated with a lithographic size of $0.6 \times 0.6\,\mu$m^2 on a $100\,\mu$m-long and $25\,\mu$m-wide GaAs/AlGaAs Hall bar with $\mu_H = 100$ m^2/Vs and $n_s = 3 \times 10^{15}/$m^2. A FIR emitter are installed in the mixing chamber of a dilution refrigerator together with the quantum-dot sample. The FIR emitter, placed at a distance of 25 mm from the sample, is a standard 2DEG Hall bar with a length and a width of $500\,\mu$m and $100\,\mu$m, respectively, which is fabricated on a high-mobility GaAs/AlGaAs heterostructure crystal similar to that used for the quantum-dot sample. It has been confirmed by an additional experiment that very weak but narrow-band FIR waves $(\lambda/\Delta\lambda = 50)$ centered at the cyclotron resonance frequency are radiated due to cyclotron emission when a current $(100\,\mu$A$)$ is passed through the Hall bar. The mixing chamber is placed in a superconducting solenoid, where the relative position of the quantum-dot sample to the solenoid is adjusted so that the CR energy of the quantum-dot sample is equal to the energy of the photons from the emitter. The FIR waves are guided through a 2 mmϕ metal light pipe to the quantum-dot sample. The FIR power reaching the area of the quantum-dot sample $(100\,\mu$m $\times 25\,\mu$m$)$ is extremely weak, roughly estimated to be of the order of 1 fW. The FIR waves are modulated by the current through the Hall-bar emitter at 20 Hz,
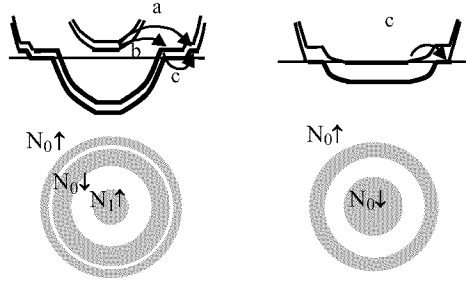
Fig 7. Illustrations of the Landau level energy profile in a three-level situation (the left) and in a two-level situation (the right).

and the photosignal is measured with a Lock-in amplifier.

Figure 5(a) illustrates Coulomb-blockade oscillations of conductance G along with the modulated conductance ΔG in the absence of magnetic field. The amplitude of the current through the emitter is adjusted so that the Joule heating is the same as that in magnetic fields. No appreciable signal is seen in ΔG, assuring that the black-body radiation from the emitter is small, and does not affect the G of the dot.

Upon application of B, definite photoresponse appears as shown in Fig. 5(b) for $B = 4.6$ T. Similar photoresponse is observed in a B-range of 4.5 T–5.4 T, where $\nu = 2.8-2.3$ in the 2DEG outside the dot. The line shape of the photoresponse versus the control gate voltage V_{CG} resembles that of the conductance change as the temperature of the quantum-dot sample is elevated, as shown in Figs. 6. The observed amplitude of the photoresponse suggests that $\Delta Te \sim 0.5$ mK, which is reasonably expected from the incident radiation power and the heat capacity of the 2DEG.

The noise equivalent power in this experiment is roughly estimated to be as low as 1×10^{-15} W$/\sqrt{\text{Hz}}$.

4   Quantum dots: single-photon detection?

One-electron states of a relatively large quantum dot (with a few hundred electrons), such as shown in Fig. 4, can be conveniently classified by the Landau level index $i \uparrow$ or $i \downarrow$ in strong magnetic fields. The left column of Fig. 7 illustrates a three-level configuration, in which the lowest three Landau levels are occupied in the dot with $N_{0\uparrow}$, $N_{0\downarrow}$, and $N_{1\uparrow}$ electrons.

Coulomb blockade peaks in strong B are affected not only by the total number of electrons N but also by the electron numbers in the respective levels [7], as described below. As B increases, electrons are transferred from higher levels to lower levels within the dot until the two-level configuration is eventually reached as shown in the right column of Fig. 7 [8, 9]. This transition proceeds as the three processes a $(1 \uparrow\to 0 \uparrow)$, b $(1 \uparrow\to 0 \downarrow)$ and c $(0 \downarrow\to 0 \uparrow)$ take place sequentially (with order unspecified). Each event of a, b, or c is associated with a polarization within the dot, and causes the electro-chemical potential of the outer-most ring $(0 \uparrow -$states$)$ to increase discontinuously. Accordingly, each event of a, b and c caused a saw-tooth like structure in the conductance G as the magnetic field is scanned; as was first demonstrated by van der Vaart et al. in the two-level case [7]. The inset of Fig. 8 illustrates an example taken on one quantum dot on the sample shown in Fig. 4, where the dot is in a conducting state
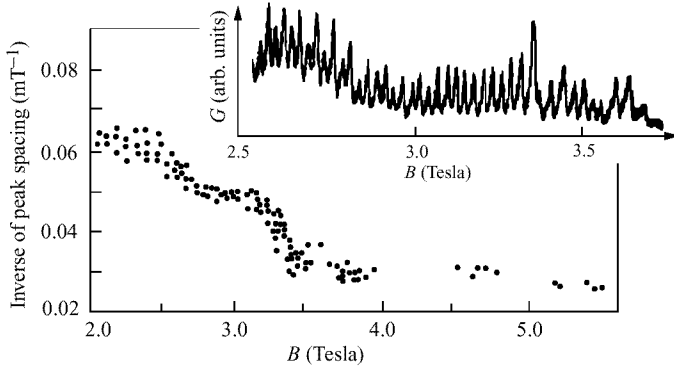
Fig. 8. Saw-tooth structures appearing in the conductance as B is scanned (the inset). Variation of the inverse of averaged spacing of the saw-tooth peaks with B.
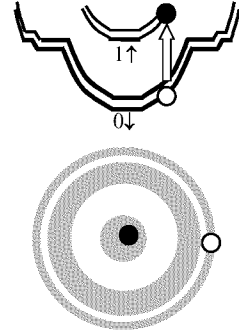
Fig. 9. Cyclotron resonance in a dot (the upper panel), resulting in a polarization between the inner core and the outer ring (the lower panel).

with a fixed voltage on the control gate.

The average spacing between the saw-tooth like peaks significantly increases as B increases. Figure 8 summarizes results of similar measurements, made with several different voltages applied on the control gate. Let r_a, r_b and r_c be the rates at which the processes a, b, and c take place per unit increase of B. Figure 8 is interpreted as representing the total rate, $r = r_a + r_b + r_c$. The total rate r decreases by about a factor of 2 as B increases to 3.4 T, above which r is substantially unchanged and takes a value of 0.03 /mT. Because the area, $S_{0\uparrow}$, surrounded by the outermost ring ($0\uparrow$ −states) is expected to be substantially unaffected by B, the sum of r_a and r_c is a constant determined by the dot size; viz., $r_a + r_c = S_{0\uparrow}/(h/e)$. The rate of event b, r_b, will decrease from $r_b = S_{0\downarrow}/(h/e) = S_{0\uparrow}/(h/e)$ to zero as the three-level configuration changes to the two-level configuration. Thus, Fig. 8 is interpreted as indicating the three-to-two-level transition in the interval of $B = 2.4\,\mathrm{T} \sim 3.4\,\mathrm{T}$. The diameter of the dot ($S_{0\uparrow}$) is evaluated to be $0.4\,\mu\mathrm{m}$ from the saturated value of $r = 0.03/\mathrm{mT}$.

Keeping the above in mind, suppose that one photon is absorbed via CR within the dot. An electron is excited in the $1\uparrow$-level leaving a hole in the $0\uparrow$-level in the three-level configuration as illustrated in the upper panel of Fig. 9. The electron and the hole will spatially depart from each other in the confining potential, release excess energies to the lattice, and eventually induce a polarization between the inner core and the outermost ring as symbolically indicated in the lower panel of Fig. 9. This is an effect equivalent to that caused by process a. This, in turn, will lead to a conductance change that can be detected in the experiments, as is expected from the data of Figs. 8.

The detection would be spoiled unless the lifetime of the induced polarization is longer than the time constant of the measurement. The lifetime may be determined by the tunneling probability of electrons between the inner core and the outer ring(s). Experiments on high-mobility 2DEG Hall bars [10] make us to speculate that the lifetime here be long, reaching the order of ms, if the dot size is not too small. The assumption of the long lifetime of the excited state of the dot is supported further by additional experiments.

When the control gate voltage is scanned at a fixed B, switching occasionally takes
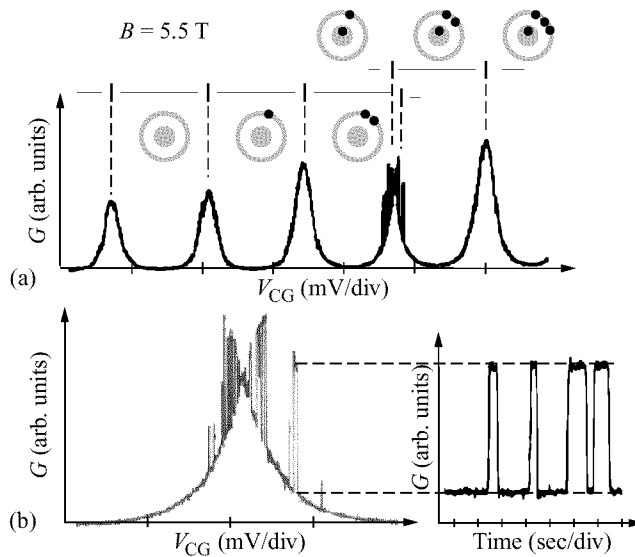
Fig 10. (a) Switching due to tunneling of a single electron between the inner core and the outer ring within the dot (the second peak from the right). (b) Magnified representation of the switching (the left) and its time dependence (the right).

place between two conductance peaks that correspond to different internal configurations [7]. Figure 10(a) displays an example taken on the same dot as that used for Fig. 8 in the two-level case. Figures 10(b) elucidates the switching between the conductance peak associated with $[N_{0\uparrow}(+1), N_{0\downarrow} + 1]$ and that associated with $[N_{0\uparrow} + 1(+1), N_{0\downarrow}]$, and shows that the switching time reaches the order of second, in agreement to the earlier report [7].

5   Discussion and conclusion

In the IQHE Hall-bar detector, the 2DEG works as an efficient absorber as well as a sensitive thermometer. In the quantum-dot detector, the 2DEG serves as an absorber while the quantum dot works as a thermometer. The performance of both types of detectors has not yet been optimized, but is among a highest level of existing detectors available in the range of FIR waves [11]. One additional merit of the IQHE Hall-bar detector is the sharp narrow-band response [3] tunable by magnetic field. Yet another merit may be the wide range of tunability. The spectral response has been studied in a magnetic field range down to 0.4 T ($\lambda = 2$ mm) [12]. The single photon detection predicted in this report may become probable when appropriate antennas structures are applied to efficiently couple a quantum dot to incident FIR waves.

Acknowledgements

References

[1] see for example, F. Thiele et al. *Solid State Commun.* **62** 841 (1987).

[2]   Yu. B. Vasiév et al. *JETP Lett.* **56** 377 (1992).

[3]   K. Hirakawa et al. *Proc. 23rd Int. Conf. Phys. of Semicond.* (Berlin, 1996, World Scientific, p. 2543).

[4]   E. Diessel et al. *Appl. Phys. Lett.* **58** 2231 (1991).

[5]   S. Komiyama et al. *Jpn. J. Appl. Phys.* **32** 4987 (1993).

[6]   E. Gornik et al. *Phys. Rev. Lett.* **54** 1820 (1985).

[7]   N. C. van Vaart et al. *Phys. Rev. B* **55** 9746 (1997).

[8]   J. P. Bird et al. *Phys. Rev. B* **49** 11488 (1994).

[9]   The total number of electrons N decreases as well with increasing B, giving rise to magneto-Coulomb oscillations [8]. However, the rate of decrease is far smaller and is ignored here.

[10] S. Komiyama and H. Nii *Physica B* **184** 7 (1993).

[11] see for example, G. Chanin and J. P. Torre, *"Infrared and Millimeter Waves"*, Chapter 5 of Vol. 10, Ed. by K. J. Button, 1983, Academic Press.

[12] V. I. Gavrilenko et al. *in this issue*.